1.0

2.8 2.5

3.2

3.6 2.2

2.0

1.1

1.8

1.25 1.4 1.6

SECURITY CLASSIFICATION OF THIS PAGE (When Data Entered)

REPORT DOCUMENTATION PAGE		READ INSTRUCTIONS BEFORE COMPLETING FORM
1. REPORT NUMBER 243-027-009	2. GOVT ACCESSION NO. AD-A098234	3. RECIPIENT'S CATALOG NUMBER
4. TITLE (and Subtitle) Single Crystal Epitaxy and Characterization of β-SiC		5. TYPE OF REPORT & PERIOD COVERED Annual Report. 1 Jan 80-31 Dec 80
		6. PERFORMING ORG. REPORT NUMBER
7. AUTHOR(s) R. F. Davis		8. CONTRACT OR GRANT NUMBER(s) N00014-79-C-0121 N00014-79-C-0121
9. PERFORMING ORGANIZATION NAME AND ADDRESS Engineering Research Services Division North Carolina State University, Burlington Laboratory, Raleigh, N. C. 27650		10. PROGRAM ELEMENT, PROJECT, TASK AREA & WORK UNIT NUMBERS PE 61153N RR 021-02-03 NR 243-027
11. CONTROLLING OFFICE NAME AND ADDRESS ONR-427 Arlington, VA 22217		12. REPORT DATE 31 March 1981
		13. NUMBER OF PAGES 136
14. MONITORING AGENCY NAME & ADDRESS(if different from Controlling Office) 16/1		15. SECURITY CLASS. (of this report) Unclassified
		15a. DECLASSIFICATION/DOWNGRADING SCHEDULE

16. DISTRIBUTION STATEMENT (of this Report)

Approved for public release; distribution unlimited

17. DISTRIBUTION STATEMENT (of the abstract entered in Block 20, if different from Report)

APR 27 1981

A

18. SUPPLEMENTARY NOTES

ONR Scientific Officer; Tel: (202) 696-4218

19. KEY WORDS (Continue on reverse side if necessary and identify by block number)

Silicon Carbide	r-f sputtering
Crystal Growth	phase Equilibria
Vapor Phase Epitaxy	

20. ABSTRACT (Continue on reverse side if necessary and identify by block number)

Single crystal thin films of β-SiC of up to five microns in thickness have been epitaxially grown on (111) Si by very carefully controlled chemical vapor deposition techniques wherein the pressure and flow rates of the reactive gases are independent of one another. Theoretical CVD phase equilibrium diagrams for the Si-C system have been calculated for various reactive and carrier gases, temperatures and pressures. A special sputtering unit has also been remodeled in order to produce amorphous SiC which can be annealed to form β-SiC or which may be used for substrates for subsequent CVD growth of this material.

DD FORM 1 JAN 73 1473 EDITION OF 1 NOV 65 IS OBSOLETE
S/N 0102-014-6601

Enclosure (1)

SECURITY CLASSIFICATION OF THIS PAGE (When Data Entered)

81 4 24 079

Annual Technical Report #243-027-009

on

SINGLE CRYSTAL EPITAXY AND CHARACTERIZATION OF
BETA SILICON CARBIDE

Submitted by

Robert F. Davis, Principal Investigator
Engineering Research Services Division
North Carolina State University
Raleigh, North Carolina 27650

I. Introduction

Silicon carbide is the only compound species that exists in the solid state in the Si-C system and can occur in the cubic (C), hexagonal (H) or rhombohedral (R) structures. It is also classified as existing in the beta and alpha modifications. The beta, or cubic, form crystallizes in the zincblende or sphalerite structure; whereas, a large number (approximately 140) of the alpha occur in the hexagonal or rhombohedral forms known as polytypes.

Because of the emerging need for high temperature, high frequency and high power electric devices, blue L.E.D.'s, Schottky diodes, U.V. radiation detectors, high temperature photocells and heterojunction devices, silicon carbide is being examined throughout the world for employment as a candidate material in these specialized applications. The electron Hall mobility of high purity undoped β-SiC is approximately a factor of three larger ($\sim$1000 cm^2/v-sec) than that of the α-form over the temperature range of 300-1000K because of the smaller amount of phonon scattering in the cubic material. The energy gap is also less in the β form (2.3 eV) compared to the α-forms (e.g., 6H = 2.86 eV). Thus, the β-form is now considered more desirable for electronic device applications, and, therefore, the growth of thin films of this material constitutes the principle objective of this research program. Unfortunately, the earlier push in the 1956-1970 time span to develop SiC as an electronic material concentrated heavily on high temperature growth processes such as the Lely sublimation-condensation technique which produced a variety of α polytypes in experiments which were rarely reproducible. Toward the end of this initial thrust, techniques such as chemical vapor deposition (CVD), sputtering, traveling solvent and solution growth showed promise not only as techniques per se but as experimental avenues wherein the growth of β-SiC could be achieved.

The objective of the present research program is to capitalize on and extend the knowledge of the CVD and sputtering processes that were discerned not only in the brief initial efforts with SiC, but that have also been developed for these processes in the intervening years in research on other semiconductor materials.

To this end, single crystal thin films of β-SiC have been successfully grown using specially designed and very closely controlled variable pressure chemical vapor deposition(C.V.D.)techniques. In addition, an adjustable target r-f sputtering unit with separately controlled gas input and pressure regulation has been redesigned around an older commercial unit. The actual retrofitting is now underway. The primary goal of this second task is to produce amorphous layers of SiC which can be used as substrates for the C.V.D. effort. Finally, a separate but a very important and an over-lapping research program involving the computer-assisted calculation of C.V.D. phase diagrams from basic thermodynamic data in the Si-C system is essentially complete. The details of these efforts and the results to date are reported below.

II. Chemical Vapor Deposition of β-SiC

A. Experimental Approach

Chemical vapor deposition is a material synthesis method in which the constitutents of the vapor phase react to form a solid film at some surface. Typical gas combinations which have been employed in the growth of SiC are CCl_4 and $SiCl_4$, SiH_4 and C_3H_8, $SiCl_4$ and C_6H_{14} and CH_3SiCl_3 alone. The complete variable pressure C.V.D. apparatus constructed inhouse and used to grow the β-SiC thin films is shown schematically in Figure 1; a brief explanation of the various lettered components is given on the succeeding page.

In the C.V.D. process, the nucleation and growth phenomena which occur at the substrate are highly influenced by the partial pressures and flow rates of each of the reactants and the carrier gas, the total pressure, the temperature of the substrates and the geometry of the reactor and the gas dynamics which this geometry helps to produce. Although it is some-what common practice to control the total pressure by controlling the flow, this technique introduces fluctuations in the gas feed which also changes the surface temperature of the substrates and the shape of the boundary layer around the sample and sample holder (a susceptor in the case of r-f heating. These changes, in turn, cause considerable fluctuations in the nucleation and growth characteristics of the deposited film and hinder the achievement of a thin film which possesses both single crystallinity and a uniform cross section.

Figure 1.   Schematic representation of the variable pressure C.V.D.
apparatus constructed for the thin film growth of β-SiC.
An explanation of the lettered components is given on the
following page.

A=Air cylinder

ABV=Auto Butterfly valve

B=Baratron pressure sensor

BB=Bunsen Burner

BC=Ball type check valve

BV=Brooks valve

C=Check valve

CC=Corrosion resistant check valve

D=Door for loading chamber

DB=Differential Box for RGA

DP=Diffusion pump

FC=Flow controller

FM=Mass flow meter

FV=Foreline valve

GV1=Auto gate valve#1

GV2=Auto gate valve #2

H= Height adjust mechanism

H2-P=H_2 purifier (Pd/Ag Diffuser)

IV=Isolation valve for Baratron

LC=Loading chamber

LCC=Liquid collection chamber

LN=Liquid nitrogen cold trap

LR=Line regulator

M=Motor

MBV=Manual butterfly valve

MGV=Manual gate valve

MSP=Molecular sieve purifier

MST=Molecular sieve trap

MV=Manual valve

N=Nutralization chamber for HCl gas

NB=Needle bearing

P=Mechanical pump

PT=Particle trap

P-T=P-trap

Q=Quartz reaction chamber

R=Rotation

R&X=Regulator and Cross purge assembly

RDBC=RGA differential box chamber

RGA=Residual Gas Analyzer

RV=Roughing valve

S=Substrates and susceptor

SSC=Stainless steel chamber

SSS=Stainless steel shaft

SST=Stainless steel tubing

SV=Solenoid valve

TC=Thermocouple gage

V=Pneumatic valve

In order to circumvent the aforementioned gas fluctuation problems, the investigators in the present program have incorporated into their system separate mechanisms for the control of flow and pressure. The control of the former employs electronic feedback loops for each gas wherein the flow rate for each gas is numerically established using separate setpoint potentiometers. The actual flow rate of each gas is measured with a Tylan flow meter, (FM),* which provides a signal to the control unit which is proportional to the flow rate. The central MKS control unit subsequently adjusts (within 0.1 msec) a magnetic valve (BV) on each gas line until the desired flow is established. Furthermore, each of the reactant gases is slaved to the carrier gas so that if any change in flow rate should occur accidentally (this has not happened as yet) or be desired by the operator, the ratio of the gases to each other will not change unless purposefully augmented by the operator at the central control unit.

Control of pressure is completely separate and accomplished by using an electronic capacitance manometer (B) which provides a signal to a control unit which, in turn, automatically opens or closes a servo-mechanical valve (ABV) to achieve the desired setpoint pressure previously established by the operator. In this way the control of pressure and flow are completely separate and result in stable gas reaction kinetics inside the CVD chamber.

Additional features of the unit include pneumatic positive shutoff valves (SV) for each gas line as well as the mixing line to compensate for the fact that the magnetic valves which precede the former valves do not completely close and therefore could allow the mixing of the gases. A check valve(C) in each of the gas lines and in the mixing line (CC) also prevent the possible mixing of gases in the individual tanks. To establish a steady flow the mixed gases are initially vented directly to the pump using a bypass line; after equilibrium is established, the mixture is switched into the chamber. The system is pumped twice to 10^{-6} torr using a liquid nitrogen trapped (LN) diffusion pump (DP) accompanied by an

---

*Symbols correspond to those shown in Figure 1.

intermediate backfill of high purity argon. During an actual run,
the gas stream flows through the two liquid nitrogen traps (used to
capture HCl which is later sublimed in a partial vacuum containing
rapidly flowing argon) into a mechanical pump into which a flow of
nitrogen is maintained to carry the gases away and therefore prevent
the possibility of a pump fire or explosion from a SiH_4-air reaction
above the oil level. The gases are exhausted through a NaOH trap (N)
to neutralize the HCl and subsequently pyrolized before the product
gases are released to the atmosphere. The system is r-f heated
(15 kw at 10 kcycles/sec), as numerous experimental efforts have shown
this technique to be superior over hot wall reactors for producing
single crystal films. The high purity graphite susceptor has been
coated in situ with SiC prior to the initial runs and is continuously
coated with this material during the actual growth processes. Finally,
the susceptor may also be pneumatically raised into the chamber or
lowered into a sample change box which can be isolated from the system,
and the latter maintained in the deposition mode.

Although this LPCVD system is at or beyond the commercial state-of-
the-art, the gas dynamics, total and partial gas pressures, temperature
and susceptor geometry must be correctly chosen in order to achieve the
growth of the desired material in a uniform manner across a substrate.
A review of the CVD literature reveals the occasional use of very low
pressures ($\leq 10^{-3}$ torr) to produce thin films; however, this may cause
more problems than it solves. The following abbreviated table provides
an indication of the increase in mean free path with a decrease in pressure.

Table I. Mean free path of air as a function of pressure

Pressure		Mean free path
torr	atm	
760	1	10^{-6} cm
1	$\approx 10^{-3}$	10^{-3} cm
10^{-3}	$\approx 10^{-6}$	5 cm

If the mean free path of the atoms becomes very long, one may not achieve chemical equilibrium in the gas stream. Equilibrium requires gas-gas collisions. If the mean free path of the gas is longer than the distance between the susceptor and the chamber wall, the gas may be pumped through without contact with the susceptor. In our case, pressures below approximately 0.05 torr would not result in chemical equilibrium.

In addition to the above, a second factor also comes into play in selecting suitable CVD pressures for the growth of SiC. The desired growth phenomena should be diffusion controlled in the gas phase in contrast to being surface reaction controlled on the substrate or being caused by the onset of homogeneous nucleation in the gas phase which results in the deposition of particulates. Several reports concerned with the growth rate of silicon from silane have shown that 1) at high temperatures, the growth is controlled by homogeneous nucleation, 2) at intermediate temperatures, it is controlled by gas phase diffusion and 3) at low temperatures the reaction rate at the surface is the controlling factor. Furthermore, the extent of the region of gas phase diffusion control _decreases_ with a _decrease_ in pressure until at 80 torr, the deposition is surface reaction controlled at all temperatures. This, 80 torr represents an approximate minimum pressure for our present effort to produce SiC since SiH_4 is the principal silicon-containing gas.

Since H_2 is our principal carrier gas (Argon has also been used), the varying solubility of carbon-containing gases in H_2 as a function of pressure and temperatures must also be taken into consideration. Lydtin has shown that the C/H ratio as a function of temperature goes through a minimum at a temperature which is directly dependent on the total pressure. To the left of this minimum the solubility continues to rise; however, to the right of the minimum, all C/H ratios eventually reach the same value, at $\approx 1575°C$ regardless of the total pressure. As we have experimentally shown that the optimum growth temperature in our system should be $\approx 1350°C$, this has also dictated that the pressure should be close to but less than one atmosphere. It is important to note that the minimums in the C/H ratio

as a function of temperature also coincide with the minimums in the area of the region of growth of β-SiC at a given temperature in the theoretical CVD diagrams discussed below. Thus, too low a pressure during the deposition may lead to serious problems in producing a well ordered single crystal thin film. This has also been borne out by our own experiments.

The carbon solubility in the gas stream also plays a definitive role in determining minimum flow rates. Although one may establish a substrate temperature which exceeds the temperature of minimum carbon concentration, the resulting gradient will contain this minimum temperature and present the possibility of homogeneous nucleation in the gas phase and the deposition of carbon particulates. To decrease the likelihood of this phenomenon, the distance between the gas boundary layer and the substrate should be reduced to push the minimum solubility close to the substrate and, therefore, reduce the amount of time allowed for the free carbon to form. The easiest way to force the boundary layer closer is to increase the gas flow rate.

The total flow rate has been increased by increasing the total amount of H_2 carrier gas going into the system. The former flow rates employed were 5-10 sccm for the reactant gases and approximately 1000 sccm for the H_2. A new 5000 sccm flow meter and valve have been installed (larger ones would exceed the capacity of the H_2 purifier) to bring about the increase. The H_2 flow rates currently employed are between 1500 and 2000 sccm while that of the reactant gases is 3-5 sccm. This has also reduced even further the partial pressures of the reactant gases which is beneficial in our case, in order to decrease the growth rate, increase the surface diffusion time and therefore increase the probability of single crystal formation. Increasing the flow rate is a superior method of decreasing the partial pressures, as the alternative of reducing the individual gas pressures and therefore the total pressure can lead to increased roughness of the surface.

An additional change in the experimental arrangement has been to move the r-f work station very close to the CVD chamber and enlarge the diameter of the copper tubing from which the induction coil is produced from 0.25 in to 0.375 in. This has allowed us to maximize the r-f efficiency

and to increase the maximum temperature measured on the substrate from 1150°C to approximately 1320°C. The temperature of the back of the Si substrates may approach 1420°C, the melting point of Si, which is the limiting factor in the current growth scenarios. This has considerably enhanced our ability to grow single crystals thin films of β-SiC. For one atmosphere CVD of SiC, a review of the literature has indicated that a temperature of 1350°C would be the minimum for obtaining single crystal SiC films. However, the moderately low pressure (380-500 torr) used in our research has allowed a decrease in this temperature, for as the partial pressures of the reactants are lowered, the growth rate is lowered and therefore, the temperature necessary for good growth may be decreased.

The combination of the aforementioned theory and practice has culminated in the following experimental conditions currently employed to grow single crystal thin films of β-SiC

Total Pressure:	380-500 Torr
Temperature:	1320°C (measured at the top surface of Si substrate; the emissivity correction is included)
Flow Rates:	(values have been taken from mass flow meter measurements; the linear flow rate in the chamber is ~21 cm/min)
H_2:	1500-2000 sccm
SiH_4:	3-5 sccm
C_2H_4:	3-5 sccm
Substrate:	(111) Si
Deposition:	20 min (~1.5 μm film is produced)
	SiC coated graphite
Susceptor Rotation Speed:	8 rpm

B. Characterization of CVD Thin Films

1. Pole Figure X-ray Analysis

A reflection type pole figure device has been employed to check the the single or polycrystallinity and the optiaxial relationships of the grown film. This equipment uses a special sample holder which allows rotation of the specimen in its own plane about an axis normal to its surface and about a horizontal axis. The sample axis which is in line with the incoming X-ray beam is initially set at ~2° which is the

approximate angle that our Si wafers deviate from the true <111> axis. This setting makes equal angles with the incident and diffracted beams.

Initially, each sample is slowly rotated about an axis orthogonal to the sample until diffraction conditions for Si occur. (In our present samples, we wish to observe and record diffraction from the (111) planes). Once this plane is located for Si, the initial Bragg angle is subsequently changed to be very close to that for the diffraction conditions of the (111) plane of β-SiC. This step determines whether or not epitaxial growth of β-SiC has occurred. In our research, epitaxial growth has been achieved as is evident by the obvious (111) β-SiC peak.

CVD structures may also grow in a fibrous manner wherein the film is formed from successively deposited layers which are polycrystalline in nature or result in single crystal fibers or pyramids. If the fiberous structure exists but the individual fibers are oriented differently in relation to one another, one may indirectly discern their presence, at least in β-SiC, by rotating the aforementioned sample 35° about the sample axis which is parallel to the incoming x-ray beam. This is the interplanar angle between the (111) and (220) planes for a diamond cubic structure. The Bragg angle is now changed to read the Si (220) peak and subsequently changed again to record the β-SiC (220) peak. If the fibers are oriented in the same way relative to each other, or if the film is single crystal, three (3) (220) peaks will be found at 120° from each other since the (11̄1) orientation has 3-fold symmetry. If the fibers are oriented randomly with respect to each other, no change in the measured intensity of the diffracted beam will be observed and polycrystallinity may be assumed. In our latest research all three (220) peaks of the β-SiC are evident indicating that the films are single crystal in nature or that any existing fibers are of the same orientation relative to one another.

In addition, a 10/2θ/min x-ray diffractometer scan of the β-SiC from 75° to 25° has not revealed the presence of Si (at least above 3wt%) as a second phase. Additional work in this area of second phases will be conducted in the coming year using back reflection Laue for long term exposures and optical microscopy.

2. Optical Microscopy

Optical examination to date has been used almost exclusively to determine the surface conditions and uniformity of the films as a function of position on the susceptor. Creating a susceptor geometry which simultaneously allows for the formation of a proper boundary layer for deposition, the correct preheater length, excellent susceptibility of the r-f field and uniform deposition across the substrates is a non-trivial design problem and, as our experience shows, necessitates many iterations. The efficacy of our various designs has been checked using optical microscopy over a range of magnifications.

Preliminary measurements of thickness have also been conducted. After 20 minutes under the conditions noted in the table of the previous section, the average thickness from top to bottom is approximately 1.5 μm. Uniformity was a particular problem for the films grown in the upper half of the susceptor; this problem was mitigated considerably as the substrates were moved down the susceptor. This latter phenomenon is believed caused by the fact that the gas is allowed to be preheated over a larger span and to establish an equilibrium boundary before it reacts with the substrates.

It should be noted that the investigators have also developed techniques for chemically removing the Si substrate from the β-SiC thin film for the purpose of transmission electron microscopy. Unfortunately, only those films 2000 Å and less can be examined and are the most difficult to handle. As a result only limited success has been achieved by this technique. Additional work in this area as well as reflection electron microscopy and scanning electron microscopy will be conducted during the next year.

3. Electrical Measurements

To date only hot probe tests have been run to determine the character of the as grown films. The undoped films have all been slightly n-type. Additional Van de Pauw experiments and optical measurements will be attempted in the very near future.

III. Theoretical Si-C CVD Phase Diagrams

CVD phase diagrams have been calculated for β-SiC formation in three distinct systems. The three systems along with the range of parameters used and summaries for each system are presented below.

System No.	Precursors	Temp. Range (K)	Pressure (atm)
I.	SiH_4, CH_4, H_2	1000-1700	10.0 to 1.0×10^{-6}
II.	$SiCl_4, CCl_4, H_2$	1400-2100	10.0 to 1.0×10^{-6}
III.	CH_3Cl_3Si, H_2 and $(CH_3)_2Cl_2Si, H_2$	1400-2100	10.0 to 1.0×10^{-6}

SYSTEM I: Regions of pure β-SiC are found over a wide range of Si/Si+C ratios, temperatures, and pressures. At $P \geq 1.0 \times 10^{-1}$ atm, these regions are found at Si/Si+C$\leq$0.5 and at T$\leq$1400K. As the concentration of carrier gas (Si/H>10.0) is increased, these regions tend to broaden to give pure β-SiC at Si/Si+C<<0.5. As pressure is decreased ($P \leq 1.0 \times 10^{-2}$ atm) a gradual reduction of the formation of β-SiC occurs at T<1400K until at $P = 1.0 \times 10^{-3}$ atm no β-SiC is found. Beta SiC formation does occur, however at Si/Si+C$\leq$0.5 for $P \leq 1.0 \times 10^{-2}$ atm and T$\geq$1500K. With further decreases in pressure ($P \leq 1.0 \times 10^{-4}$ atm) there is also formation of β-SiC at Si/Si+C>0.5, and T$\geq$1500K. By adding larger amounts of carrier gas there is a broadening of pure β-SiC regions at all temperatures and pressures. The CVD phase diagrams for this portion of the research were provided in the reports of the previous year and will not be repeated here. This text has been presented to provide continuity with the remaining discussion.

SYSTEM II: In this system pure β-SiC is found at all pressures for a Si/SiC>0.5 and a carrier gas concentration equal to 10.0 moles H_2 (see Figs. 1-8). As pressure is decreased at T>1800K (with carrier gas = 10.0 moles H_2), the area of pure β-SiC formation begins to narrow (see Figs. 1-6). This region of pure β-SiC disappears under the conditions of T$\geq$1900K and $P = 1.0 \times 10^{-5}$ atm (Fig. 7), and T$\geq$1750K at $P = 1.0 \times 10^{-6}$ atm (Fig. 8).

As the carrier concentration is increased to 50.0 moles H_2, we find β-SiC at Si/Si+C<0.5 for P=10.0 and 1.0 atm as shown in Figs. 9 and 10. Upon further stepwise decreases in pressure ($P \leq 1.0 \times 10^{-1}$ atm), the β-SiC region disappears at Si/Si+C<0.45 (see Figs. 11 and 12). At T>1725K and $P \leq 1.0 \times 10^{-3}$ atm there is a gradual reduction of the pure β-SiC region, as

shown in Figs. 13-16, until at $P=1.0 \times 10^{-6}$ atm the pure β-SiC region ceases to exist.
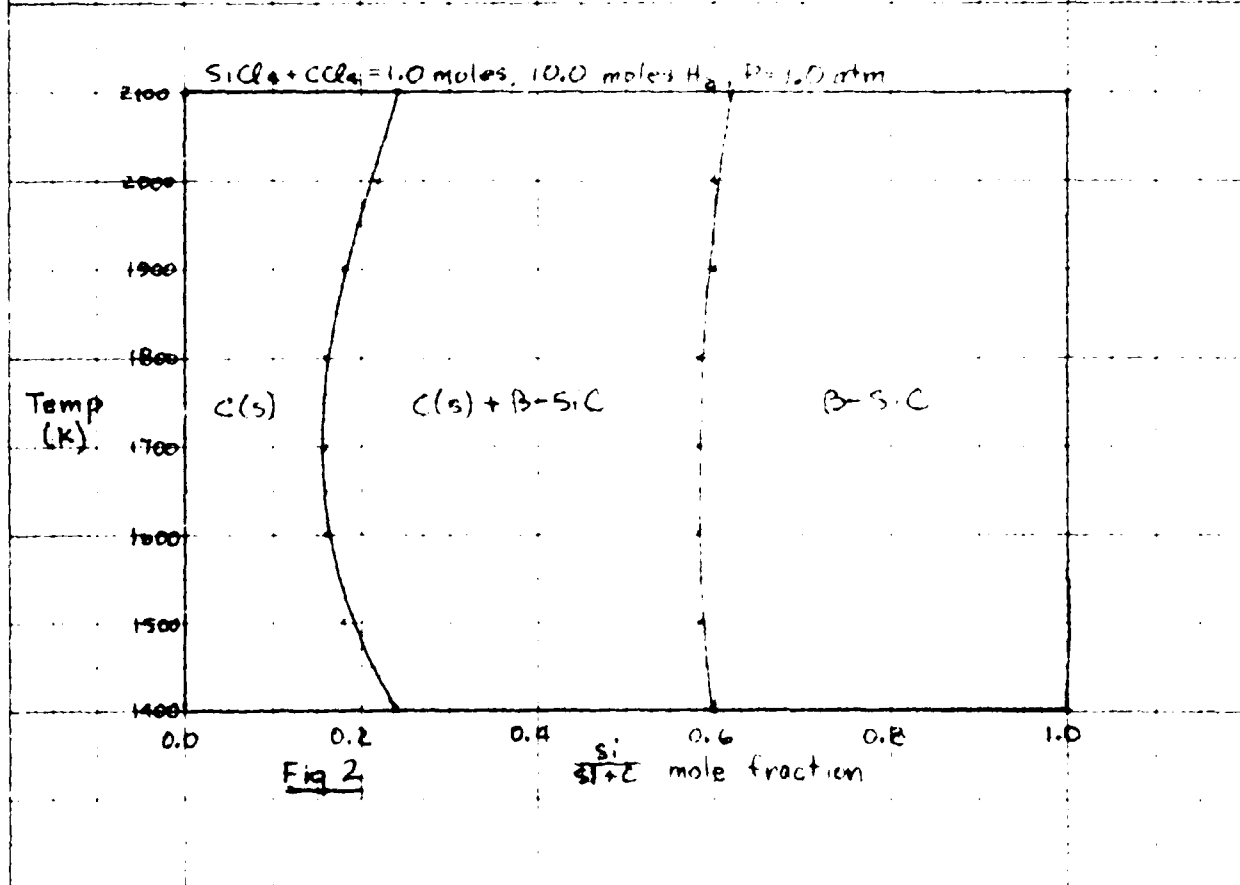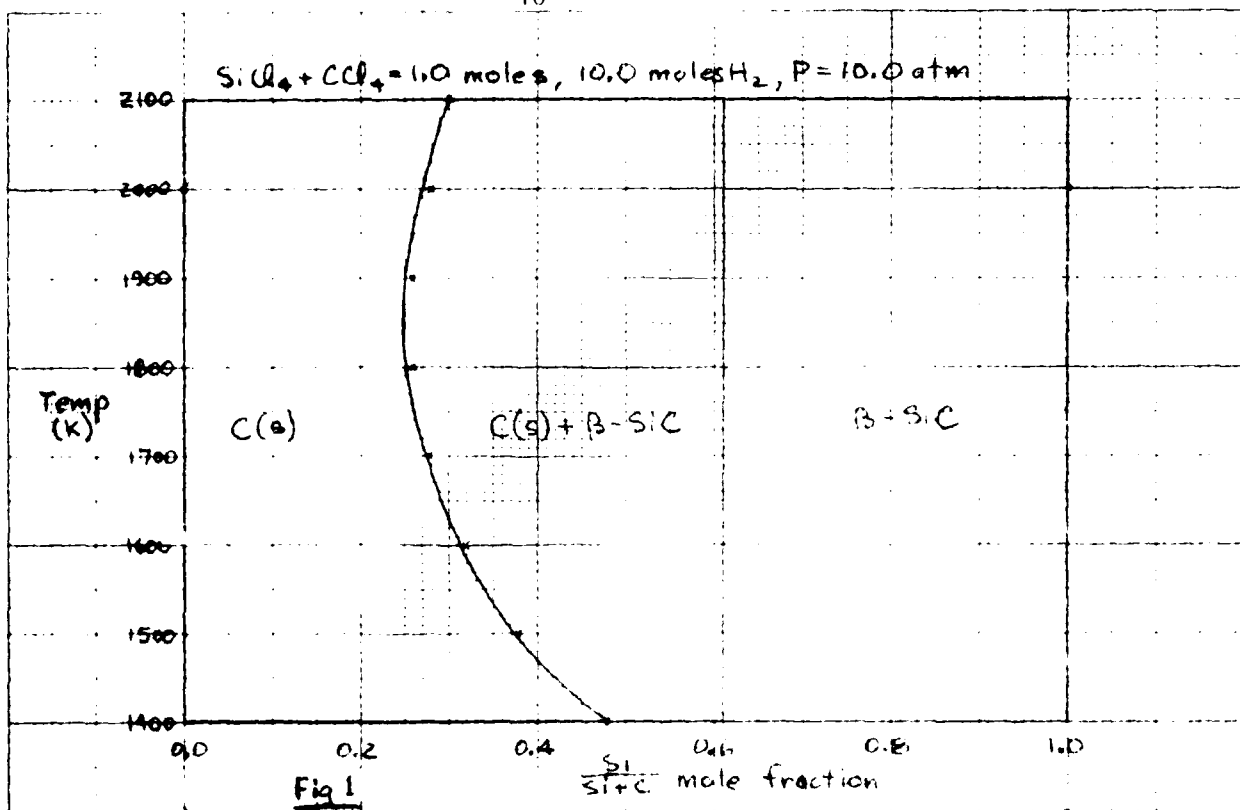
As the carrier gas concentration is increased to 100.0 moles H_2 (Figs. 17-24), the same trends as occurred with the carrier gas concentration equal to 50.0 moles H_2 are again evident. Since the H_2 reacts with the chlorine in the $SiCl_4$ and CCl_4 to give HCl, these large amounts of H_2 (in excess of what is stoichometrically required for HCl) act similarly to an inert gas.
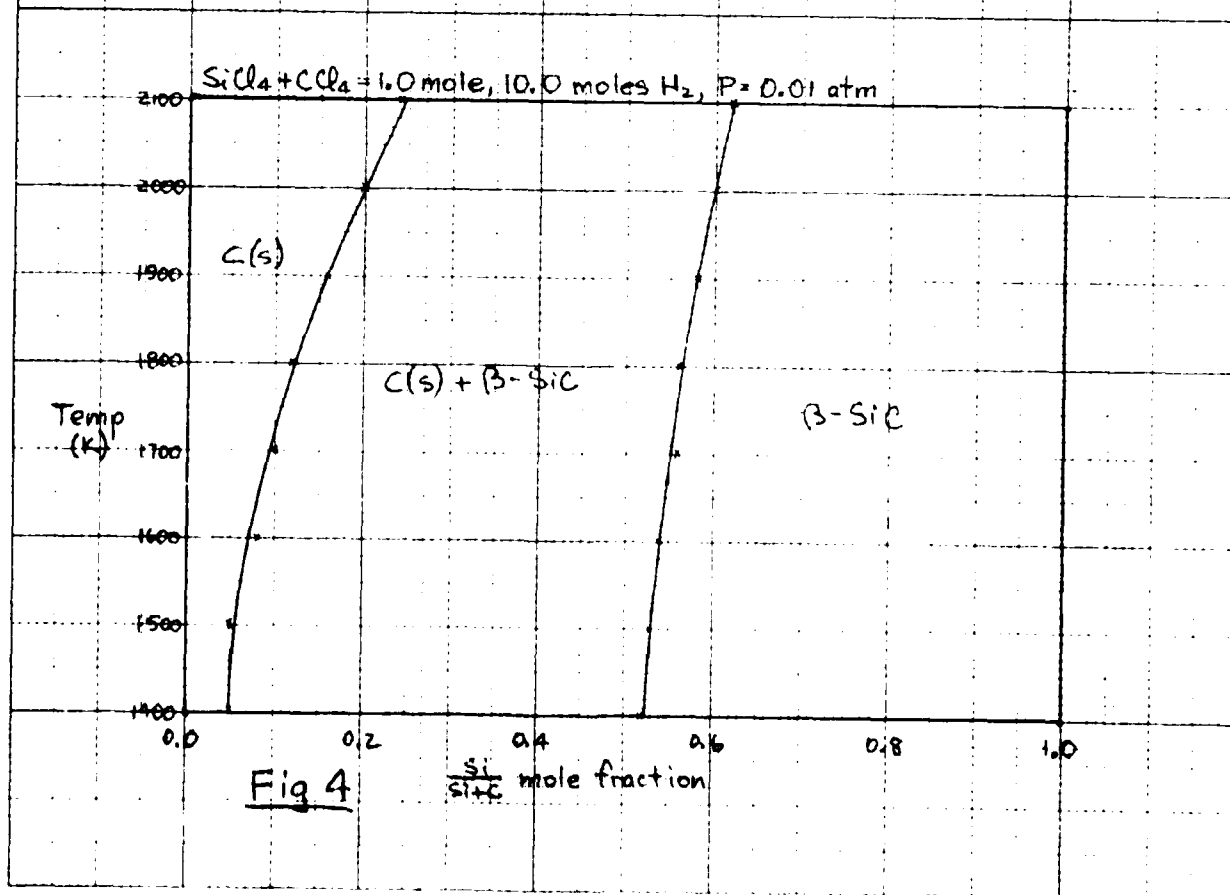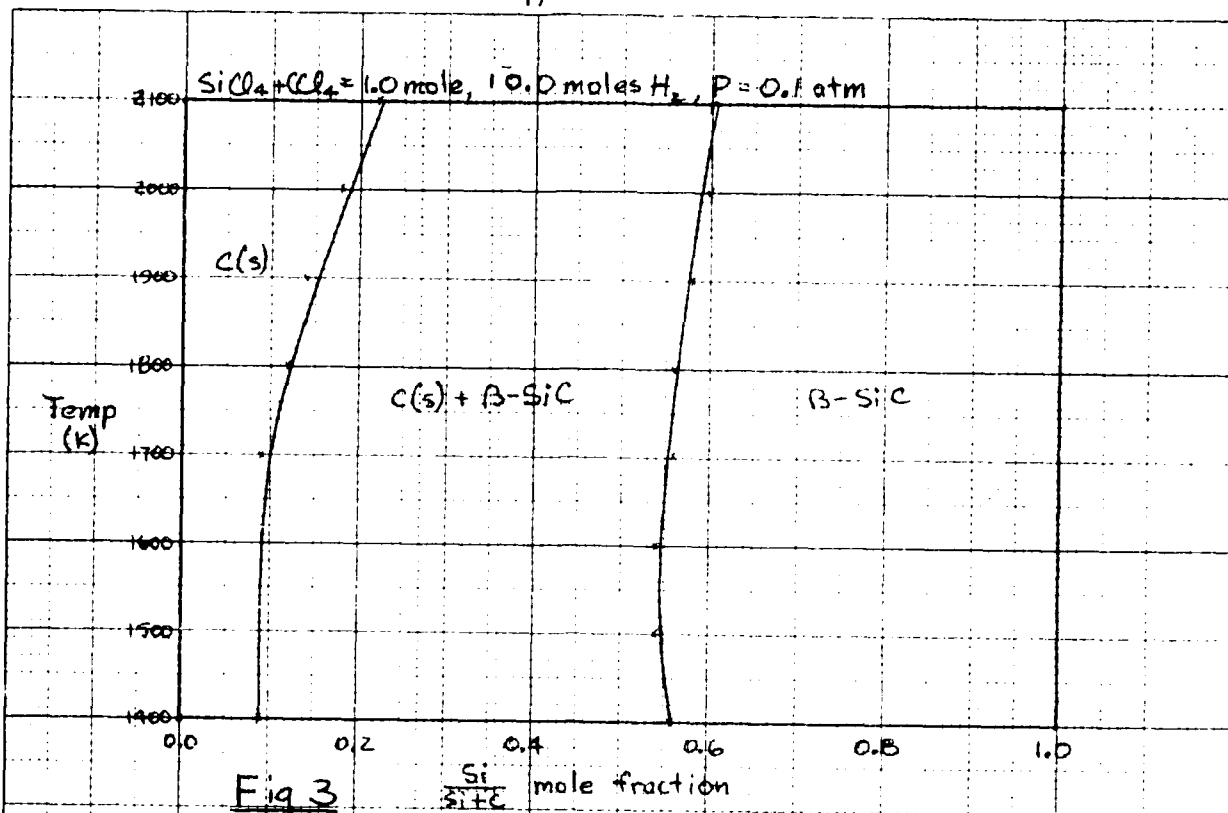
SYSTEM III. The CVD decomposition diagrams of CH_3Cl_3Si and $(CH_3)_2Cl_2Si$ in the presence of H_2 as a carrier gas were computed for two concentrations of H_2 with the pressure ranging from 10.0 atm to 1.0×10^{-6} atm (see Figs. 25-28). For 1.0 mole $CH_3Cl_3Si+50.0$ moles H_2 (Fig. 28), pure β-SiC formed at all pressures above 5.0×10^{-2} atm for the T range of 1400 to 2100K. There was no free Si formation at any temperature and pressure using 1.0 mole $CH_3Cl_3Si+10.0$ moles H_2 (Fig. 26). The only region of pure β-SiC was for $T \leq 1500K$ for $P \, 6.0$ atm; again there was no free Si formation.
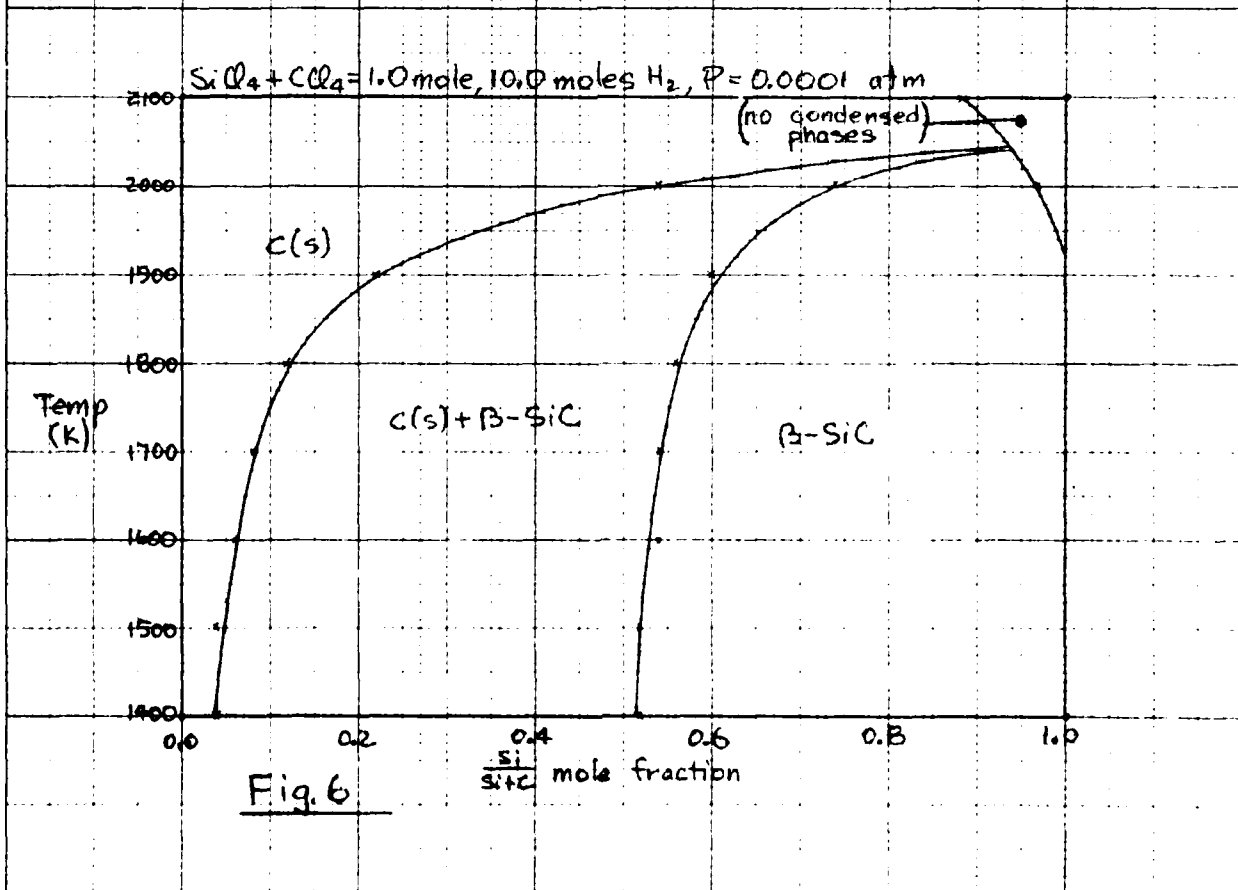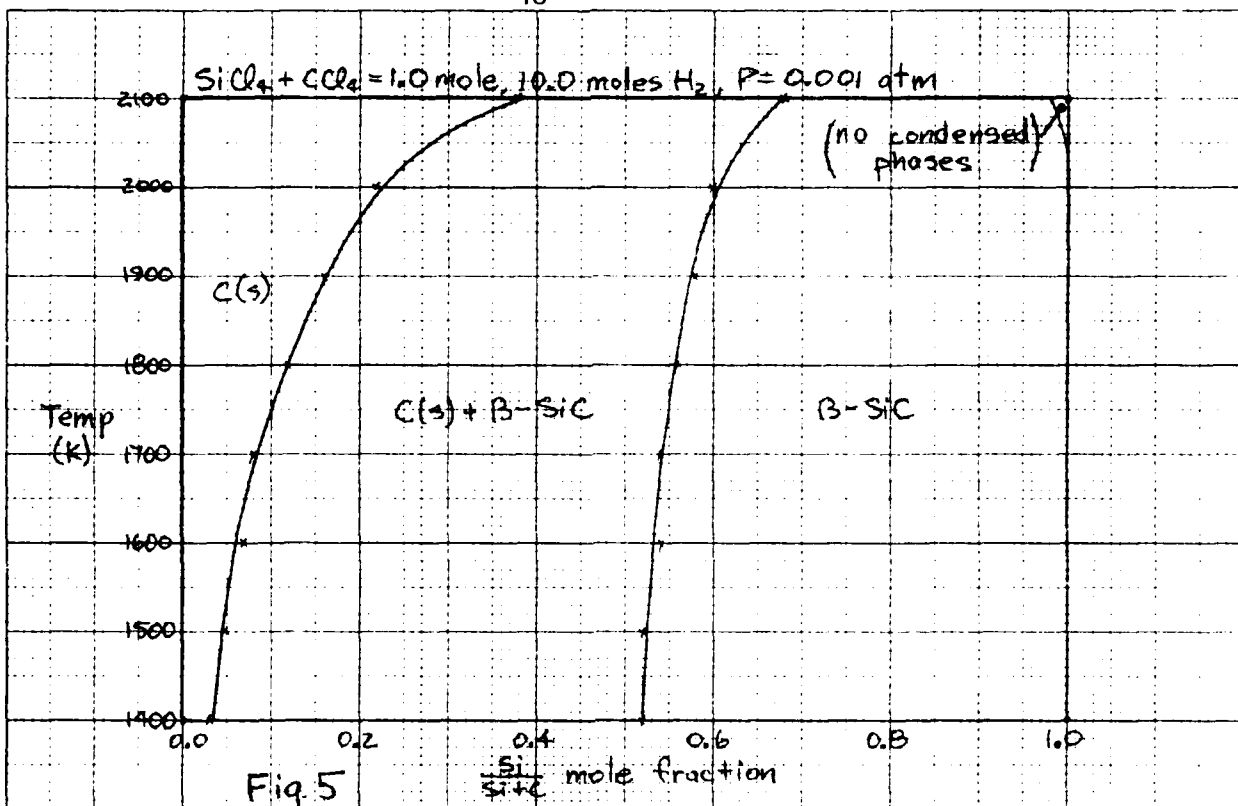
The CVD diagrams for the decomposition of 1.0 mole $(CH_3)_2Cl_2Si$ with either 50.0 moles H_2 or 10.0 moles H_2 (Figs. 25 and 27), are similar to the $CH_3Cl_3Si+10.0H_2$ diagram (Fig. 26), except that there is no region of pure β-SiC within the diagram of 1.0 $(CH_3)_2Cl_2Si+10.0$ moles H_2. Additionally, in the region of β-SiC+C the β-SiC/C ratio is lower for the $(CH_3)_2Cl_2Si$ decomposition than that for the CH_3Cl_3Si decomposition. In other words, the excess carbon of the dimethyldichlorosilane-containing gas deposits as C to a greater degree than in the methyltrichlorosilane-containing gas.

The temperature range for the SiH_4 system differs from that used for the $SiCl_4$, CH_3Cl_3Si, and $(CH_3)_2Cl_2Si$ system because SiH_4 decomposes at a much lower temperature relative to the other systems under investigation.

These summaries and graphs represent a compilation of all the CVD diagram research completed to date. Future objectives include: calculations using non-inert substrates such as SiC, Si and C; the incorporation of geometric considerations and thermodynamic constraints to yield CVD diagrams that give more of a dynamic slant to the systems under consideration.

Fig 1

$SiCl_4 + CCl_4 = 1.0$ moles, 10.0 moles H_2, P = 10.0 atm

Temp (K)

C(s)   C(s) + β-SiC   β-SiC

$\frac{Si}{Si+C}$ mole fraction

Fig 2

$SiCl_4 + CCl_4 = 1.0$ moles, 10.0 moles H_2, P = 1.0 atm

Temp (K)

C(s)   C(s) + β-SiC   β-SiC

$\frac{Si}{Si+C}$ mole fraction

461240

Fig 3 $\frac{Si}{Si+C}$ mole fraction

$SiCl_4 + CCl_4 = 1.0$ mole, 10.0 moles H_2, $P = 0.1$ atm

C(s)

C(s) + β-SiC

β-SiC

Temp (K)

Fig 4 $\frac{Si}{Si+C}$ mole fraction

$SiCl_4 + CCl_4 = 1.0$ mole, 10.0 moles H_2, $P = 0.01$ atm

C(s)

C(s) + β-SiC

β-SiC

Temp (K)

Fig. 5

$SiCl_4 + CCl_4 = 1.0$ mole, 10.0 moles H_2, $P = 0.001$ atm

(no condensed phases)

C(s)

C(s) + β-SiC

β-SiC

Temp (k)

$\frac{Si}{Si+C}$ mole fraction

Fig. 6

$SiCl_4 + CCl_4 = 1.0$ mole, 10.0 moles H_2, $P = 0.0001$ atm

(no condensed phases)

C(s)

C(s) + β-SiC

β-SiC

Temp (k)

$\frac{Si}{Si+C}$ mole fraction

Fig 7

$SiCl_4 + CCl_4 = 1.0$ mole, 10.0 moles H_2, $P = 0.0001$ atm

C(s)

n.c.p.

C(s) + β-SiC

β-SiC

Temp (k)

$\frac{Si}{Si+C}$ mole fraction

Fig 8

$SiCl_4 + CCl_4 = 1.0$ mole, 10.0 moles H_2, $P = 0.000001$ atm

C(s)

n.c.p.

C(s) + β-SiC

β-SiC

Temp (k)

$\frac{Si}{Si+C}$ mole fraction

46 1240

$SiCl_4 + CCl_4 = 1.0$ mole, 50.0 mole H_2, $P = 10.0$ atm

β-SiC + S(ℓ)

C(s)

β-SiC + C(s)

β-SiC

ncp

ncp

Temp (K)

2100 2000 1900 1800 1700 1600 1500 1400

0.0   0.2   0.4   0.6   0.8   1.0

Fig 9 $\frac{Si}{Si+C}$ mole fraction

$SiCl_4 + CCl_4 = 1.0$ mole, 50.0 moles H_2, $P = 1.0$ atm

C

β-SiC + C

β-SiC + Si

β-SiC

Temp (K)

2100 2000 1900 1800 1700 1600 1500 1400

0.0   0.2   0.4   0.6   0.8   1.0

Fig 10 $\frac{Si}{Si+C}$ mole fraction

$SiCl_4 + CCl_4 = 1.0$ moles, 50.0 moles H_2, P = 0.1 atm

C

β-SiC + C β-SiC β-SiC + Si

Temp (K)

2100
2000
1900
1800
1700
1600
1500
1400

0.0   0.2   0.4   0.6   0.8   1.0

$\frac{Si}{Si+C}$ mole fraction

Fig 11

$SiCl_4 + CCl_4 = 1.0$ mole, 50.0 moles H_2, P = 0.01 atm

C

ncp

β-SiC + C β-SiC β-SiC + Si

Temp (K)

2100
2000
1900
1800
1700
1600
1500
1400

0.0   0.2   0.4   0.6   0.8   1.0

$\frac{Si}{Si+C}$ mole fraction

Fig 12

46 1240

K°E KEUFFEL & ESSER CO

Fig 13

$\frac{Si}{Si+C}$ mole fraction

$SiCl_4 + CCl_4 = 1.0$ mole, 50.0 moles H_2, $P = 0.001$ atm

C

ncp

β-SiC+C

β-SiC

β-SiC+Si

Fig 14

$\frac{Si}{Si+C}$ mole fraction

$SiCl_4 + CCl_4 = 1.0$ mole, 50.0 moles H_2, $P = 0.0001$ atm

C

ncp

β-SiC+C

β-SiC

β-SiC+Si

Fig 15

$SiCl_4 + CCl_4 = 1.0$ mole, 50.0 moles H_2, P: 0.00001 atm

Temp (K)

ncp

C

β-SiC

β-SiC + C

β-SiC + Si

$\frac{Si}{Si+C}$ mole fraction

Fig 16

$SiCl_4 + CCl_4 = 1.0$ mole, 50.0 mole H_2, P: 0.000001 atm

Temp (K)

ncp

C

β-SiC

β-SiC + C

β-SiC Si

$\frac{Si}{Si+C}$ mole fraction

Fig 17

$SiCl_4 + CCl_4 = 1.0$ mole, 100.0 mole H_2, $P = 1.0$ atm

$\frac{Si}{Si+C}$ mole fraction

Fig 18

$SiCl_4 + CCl_4 = 1.0$ mole, 100.0 mole H_2,

$\frac{Si}{Si+C}$ mole fraction

$SiCl_4 + CCl_4 = 1.0$ mole, 100.0 moles H_2, $P = 0.1$ atm

C

$\beta - SiC + C$

$\beta - SiC$

$\beta - SiC + Si$

Temp (K)

Fig 19 $\frac{Si}{Si+C}$ mole fraction

$SiCl_4 + CCl_4 = 1.0$ mole, 100.0 moles H_2, $P = 0.01$ atm

C

ncp

$\beta - SiC$

$\beta - SiC + C$

$\beta - SiC + Si$

Temp (K)

Fig 20 $\frac{Si}{Si+C}$ mole fraction

Fig 21

$SiCl_4 + CCl_4 = 1.0$ mole, 100.0 mole H_2, P= 0.001 atm

$\frac{Si}{Si+C}$ mole fraction

Fig 22

$SiCl_4 + CCl_4 = 1.0$, 100.0 mole H_2, P= 0.0001 atm

$\frac{Si}{Si+C}$ mole fraction

Fig 23

Fig 24

Decomposition of $(CH_3)_2Cl_2Si * 1.0$ mole and $H_2 * 50.0$ moles

Fig 25

Decomposition of 1.0 mole CH_3Cl_3Si and 10.0 moles H_2

$\beta-SiC$

$\beta-SiC + C(s)$

$C(s)$

Log P(atm)

Fig 26

Temp (K)

Decomposition of 1.0 mole $(CH_3)_2 Cl_2 Si$ and 10.0 moles H_2.

$\beta - SiC + C(s)$

$C(s)$

Temp (K)

Log P (atm)

Fig 27

Decomposition of 1.0 moles CH_3Cl_3Si and 50.0 moles H_2

β-SiC

$C(s)$

β-SiC + $C(s)$

Log P (atm)

Temp (K)
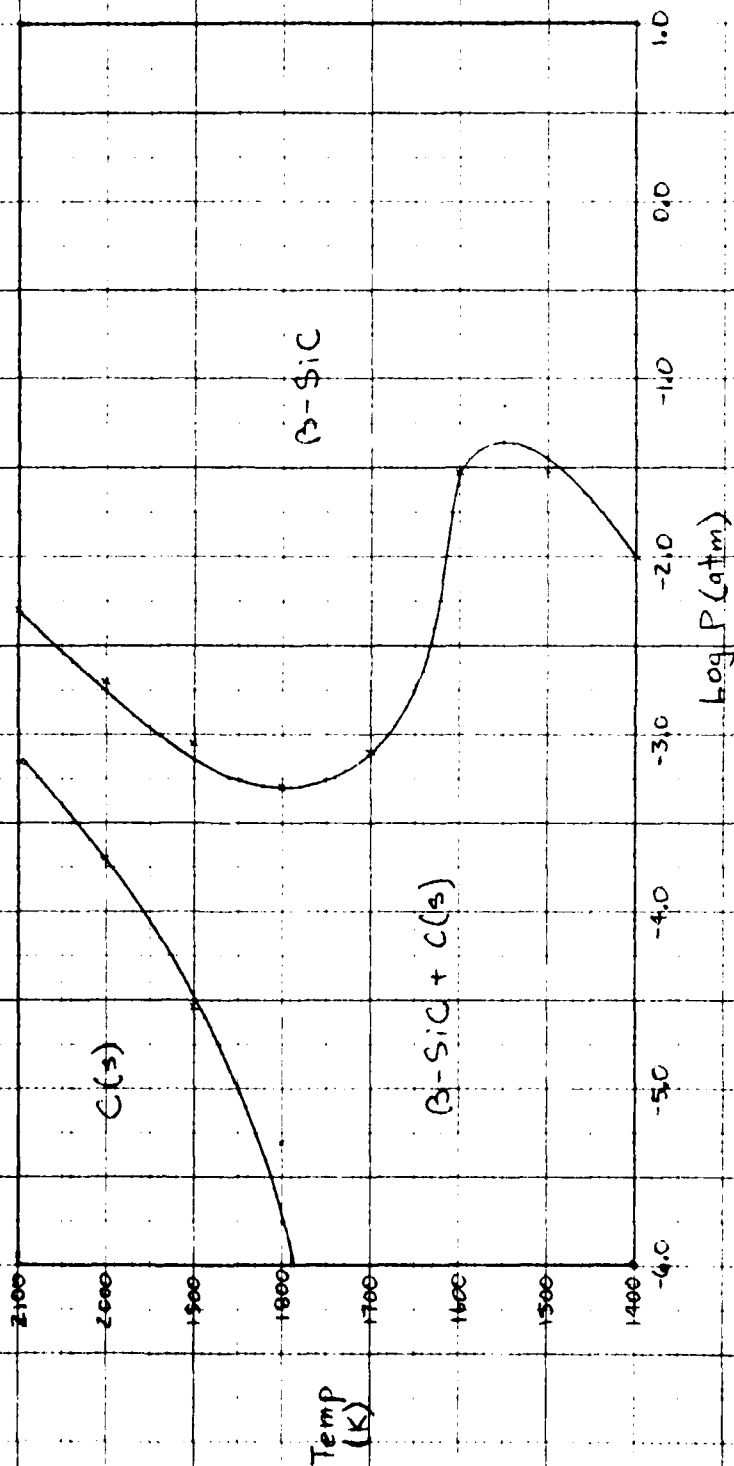
Fig 28

IV. RF Sputtering Facility

Another major effort during this past year has been the design of an adjustable target r-f sputtering unit with separately controlled gas input and pressure regulation around the pumping system, 2.5 kv power supply and tuning networks of an older commercial unit. As in the case of our chemical vapor deposition unit, we have chosen to independently control both the flow rate of the entry gas (or gases, if reactive sputtering is employed) and pressure with the use of mass flow transducers and an automatically controlled servo-mechanical valve, respectively. The valve is actuated in response to a difference between the desired setpoint pressure and that determined by a capacitance manometer. The reason for this arrangement is to avoid fluctuations in the sputtering rate and therefore the nucleation rate of the growing film which can easily lead to the growth of a polycrystalline film.

We have also designed a special β-SiC target which has been grown by chemical vapor deposition by Deposits and Composites Corporation of Reston, VA. This target is considerably superior in purity and density to that of any other type of commercial α or β SiC. Because of this unorthodox request for a very thick (by CVD standards) and rather large diameter (S) SiC disk, the company had to make several changes in their fabrication procedures. As such the target has only been recently received after a period of approximately five months.

Members of the SiC thin film group have also designed and are currently fabricating a special substrate heater which employs three 500 w quartz lamps. This heater will also be used as an anode to bias the plasma and etch the substrates.

Additional repair and retrofitting still remains to be conducted in order to fully implement our design; however, the work is proceeding smoothly and we now anticipate a start-up date of April.

V. Summary

Single crystal thin films of β-SiC having a thickness of 5 µm or less have been epitaxially grown on (111) Si by very carefully controlled chemical vapor deposition techniques wherein the pressure and flow rates of the reactive gases (SiH_4 and C_2H_4), carrier gas (H_2) and the pressure are independently controlled. Analyses of 1) the mean free path of the reactive gases,

2) the temperature and pressure regimes wherein the deposition of Si and the subsequent growth of β-SiC are controlled by gas phase diffusion and 3) the solubility of a carbon-containing gases in H_2 and their reaction efficiency at various temperatures have led us to the use of moderate pressures (380-500 Torr) and temperatures (.1320°C) in order to achieve the single crystal films.

In addition a substantial number of theoretical CVD phase equilibrium diagrams for the Si-C system have been calculated for various reactive and carrier gases, temperatures and pressures. The single phase fields of β-SiC in these diagrams vary markedly as the aforementioned parameters change and indicates a number of reasons why several investigators have been unsuccessful in obtaining films of pure β-SiC.

Finally, a rather extensive redesign and retrofitting of a older commercial rf sputtering unit is underway. An adjustable cathode (target) wherein the cathode-anode separation may be changed over large distances, a state-of-the-art substrate heater system, separate control of gas flow and pressure, and the employment of a high purity β-SiC target grown by CVD techniques are a few of the many changes now underway in order to deposit amorphous films of SiC directly on Si substrates.

Office of Naval Research Code 427Y 800 North Quincy Street Arlington, VA 22217	4	Commandant 1 Marine Corps Scientific Advisor (Code AX) Washington, DC 20380

Naval Research Laboratory
4555 Overlook Avenue, S.W.
Washington, DC 20375
Attn: Code 6812   1
          6820   2

Commander, AFAL   1
AFAL/DHM
Mr. Richard L. Remski
Wright-Patterson AFB, OH 45433

Defense Documentation Center 12
Building 5, Cameron Station
Alexandria, VA 22314

Professor Walter Ku   1
Phillips Hall
Cornell University
Ithaca, NY 14853

Dr. Y. S. Park   1
AFAL/DHR
Building 450
Wright-Patterson AFB
Ohio 45433

Commander   1
Harry Diamond Laboratories
Mr. Horst W. A. Gerlach
2800 Powder Mill Road
Adelphia, MD 20783

ERADCOM   1
DELET-M
Fort Monmouth, NJ 07703

Advisory Group on Electron Devices 1
201 Varick Street, 9th Floor
New York, NY 10014

Dr. Harry Wieder   1
Naval Ocean Systems Center
Code 922
271 Catalina Blvd.
San Diego, CA 92152

Professor L. Eastman   1
Phillips Hall
Cornell University
Ithaca, NY 14853

Professors Hauser and Littlejohn   1
Department of Electrical Engr.
North Carolina State University
Raleigh, North Carolina 27607

Dr. William Lindley   1
MIT
Lincoln Laboratory
F124A, P.O. Box 73
Lexington, MA 02173

Dr. R. S. Feigelson   1
Center for Materials Research
Stanford University
Stanford, CA 94305

Mr. Sven Roosild   1
DARPA/DSO
1400 Wilson Blvd
Arlington, VA 22209

Dr. Y. Kim   1
ONR Scientific Liaison Group
American Embassy
A.P.O. San Francisco 96503

Commander   1
U.S. Army Electronics Command
V. Gelnovatch
(DRSEL-TL-IC)
Fort Monmouth, NJ 07703

Enclosure (1)

ATE
LMED
-8